Neurobiology of Aging 106 (2021) 68–79

Contents lists available at ScienceDirect

Neurobiology of Aging

journal homepage: www.elsevier.com/locate/neuaging.org

Age- and gender-related differences in brain tissue microstructure revealed by multi-component T_2 relaxometry

Erick Jorge Canales-Rodríguez[a,b,c,*], Silvia Alonso-Lana[a,b,d], Norma Verdolini[a,b,e], Salvador Sarró[a,b], Isabel Feria[a,f], Irene Montoro[g,h,i], Beatriz Garcia-Ruiz[g,h,i], Esther Jimenez[b,e], Cristina Varo[b,e], Auria Albacete[a,b], Isabel Argila-Plaza[a], Anna Lluch[g,h], C. Mar Bonnin[e], Elisabet Vilella[g,h,i,b], Eduard Vieta[b,e], Edith Pomarol-Clotet[a,b,1], Raymond Salvador[a,b,1]

[a] FIDMAG Germanes Hospitalàries Research Foundation, Sant Boi de Llobregat, Barcelona, Spain
[b] Mental Health Research Networking Center (CIBERSAM), Madrid, Spain
[c] Signal Processing Laboratory (LTS5), École Polytechnique Fédérale de Lausanne (EPFL), Lausanne, Switzerland
[d] Research Center and Memory Clinic, Fundació ACE, Institut Català de Neurociències Aplicades, Universitat Internacional de Catalunya, Barcelona, Spain
[e] Bipolar and Depressive Disorders Unit, Hospital Clinic, Institute of Neurosciences, University of Barcelona, IDIBAPS, Barcelona, Spain
[f] Benito Menni CASM, Sant Boi de LLobregat, Barcelona, Spain
[g] Hospital Universitari Institut Pere Mata, Reus, Spain
[h] Institut d'Investigació Sanitària Pere Virgili (IISPV)-CERCA, Reus, Spain
[i] Universitat Rovira i Virgili (URV), Reus, Spain

ARTICLE INFO

Article history:
Received 2 December 2020
Revised 30 May 2021
Accepted 1 June 2021
Available online 10 June 2021

Keywords:
Brain
Aging
Tissue Microstructure
Multi-exponential relaxation
Myelin water fraction

ABSTRACT

In spite of extensive work, inconsistent findings and lack of specificity in most neuroimaging techniques used to examine age- and gender-related patterns in brain tissue microstructure indicate the need for additional research. Here, we performed the largest Multi-component T_2 relaxometry cross-sectional study to date in healthy adults (N = 145, 18–60 years). Five quantitative microstructure parameters derived from various segments of the estimated T_2 spectra were evaluated, allowing a more specific interpretation of results in terms of tissue microstructure. We found similar age-related myelin water fraction (MWF) patterns in men and women but we also observed differential male related results including increased MWF content in a few white matter tracts, a faster decline with age of the intra- and extra-cellular water fraction and its T_2 relaxation time (i.e. steeper age related negative slopes) and a faster increase in the free and quasi-free water fraction, spanning the whole grey matter. Such results point to a sexual dimorphism in brain tissue microstructure and suggest a lesser vulnerability to age-related changes in women.

1. Introduction

The female and male brains are known to develop and age differently, showing anatomical, functional, and biochemical differences in all stages of life (Zaidi, 2010). To properly interpret and design ongoing and future clinical imaging studies it is important to understand the differential impact of age and gender on brain tissue. Several volumetric studies using Magnetic Resonance Imaging (MRI) have reported sex- and age-related differences (Coffey et al., 1998). Global anatomical differences between women and men were found in a sample of healthy controls (N = 200, mean age, 21.6 years) showing that, on average, the male brain is larger and has a smaller percentage of grey matter (GM) (Leonard et al., 2008). This latter finding is in agreement with other studies employing additional metrics to charac-

* Corresponding author at: FIDMAG Germanes Hospitalàries Research Foundation, C/ Dr. Antoni Pujadas 38, Sant Boi de Llobregat, Barcelona, 08830 Spain. Signal Processing Laboratory (LTS5), EPFL-STI-IEL-LTS5, Station 11, CH-1015 Lausanne, Switzerland.
E-mail address: erick.canalesrodriguez@epfl.ch (E.J. Canales-Rodríguez).
[1] Joint last author (shared senior authorship)

0197-4580/$ – see front matter
https://doi.org/10.1016/j.neurobiolaging.2021.06.002

terize the GM morphology. For example, a cortical thickness analysis in a sample of healthy individuals (N = 176, age range, 7–87 years) revealed thicker cortices up to 0.45 mm in women than in men in the right inferior parietal and posterior temporal regions (Sowell et al., 2007). Another study in healthy youths (N = 1189, age range, 8–23 years) found that women have higher GM density than males throughout the brain (Gennatas et al., 2017).

To characterize the regional and tissue-class specificity of the brain volume changes with age, a longitudinal study analyzed a cohort of healthy aged participants (N = 122, age range, 58–95 years) using voxel-based morphometry (VBM) (Smith et al., 2007). Regression analyses showed a global GM volume decrease at a rate of -0.18% per year, a total cerebrospinal fluid (CSF) increase by 0.20% per year, and a no significant decrease in the total white matter (WM) volume; although a focal WM decrease with age was detected in the anterior part of the corpus callosum (CC) (Smith et al., 2007). More recently, a longitudinal study of regional brain volumes (17 boys and 12 girls, age range 10–14 years, and 55 men and 67 women, age range 20–85 years) reported rises in ventricular and Sylvian fissure volumes; declines in selective cortical volumes; little effect of aging on the CC volume; and more rapid expansion of CSF-filled spaces in men than women (Pfefferbaum et al., 2013).

Given the established dependence of global and regional brain volumes on gender and age, the question of how this dependence is sustained at the microstructure level has been addressed by various research groups. A diffusion tensor imaging (DTI) study (N = 135, mean age, 25 years) using the Fractional Anisotropy (FA) index detected gender differences in the WM microstructure (Kanaan et al., 2012). Specifically, higher FA in cerebellar WM and the superior longitudinal fasciculus was observed in men, whilst women had a higher FA in the CC. However, as noted by the authors, previous studies disagreed on the direction of the observed differences (Bava et al., 2011; Liu et al., 2010; Westerhausen et al., 2003), making it difficult to reconcile these findings. Another DTI study (N = 63, age range, 18–50 years) reported WM microstructure differences between individuals as a function of sex and intelligence. Interestingly, while in men higher intelligence was related to higher FA and lower radial diffusivity (RD) in the CC, in women this relationship was not significant (Dunst et al., 2014). The authors suggested that higher FA and lower RD could be explained by higher myelination and/or a larger number of axons in men. More recently, in a multimodal study combining DTI and proton density scans an approximated approach for measuring the g-ratio in the CC was proposed (N = 92, age range, 7–81 years) (Berman et al., 2018). The estimated g-ratio, defined as the ratio between the inner and outer radii of myelinated axons, was found to be relatively stable with age, and no support for a significant sexual dimorphism was found. A recent study (N = 116, age range, 45–72 years) using neurite orientation dispersion and density imaging (NODDI), an advanced multi-compartment diffusion MRI technique, reported widespread increases in the volume fraction of the free-water compartment, and localized decreases in neurite density with age in frontal white matter regions (Merluzzi et al., 2016).

However, despite the proven sensitivity of these neuroimaging techniques, many of them are unspecific. The most widely used methods to study the brain tissue microstructure – VBM (Ashburner and Friston, 2000) and DTI (Basser et al., 1994) – do not allow us to unambiguously identify the tissue compartment or the biological parameter underlying the observed changes. On the one hand, the nature of the GM and WM changes identified with VBM in healthy participants is poorly understood because the reported amount of tissue per voxel, often referred to as 'density' or 'concentration', should not be confused with cell packing density as measured by counting cell bodies (Mechelli et al., 2005). On the other hand, DTI-derived metrics like FA and RD, depend on various microstructure parameters (Beaulieu, 2002) including microscopic fiber dispersion, inter-fiber angle in fiber crossing regions, cell permeability, intercompartmental water exchange, cell packing density, and distribution of axonal diameters (Jones and Cercignani, 2010). As a result, interpreting findings from solely DTI and/or VBM metrics in terms of issue microstructure is risky. We note that despite the improved specificity provided by more advanced diffusion MRI models such as NODDI (Zhang et al., 2012), there are still important confounding factors not fully modeled. For example, NODDI is based on assuming both a constant axial diffusivity for all brain voxels (and for all participants independently of their ages) and the same T_2 relaxation time for the different tissue compartments (i.e., intra-axonal, extra-axonal, and CSF). Hence, any relationship of these non-modeled parameters with age or sex may affect the interpretation of the estimated parameters.

A potentially useful technique for characterizing the microstructure of different tissue compartments is multi-component T_2-relaxometry. This technique allows obtaining quantitative information about the transverse relaxation times and water volume fractions of various cell compartments from multi-echo T_2 MRI data. It is considered as the gold standard to compute the myelin water fraction (MWF) (Alonso-Ortiz et al., 2015), a metric highly correlated with the volume of the myelin tissue (Laule et al., 2008). Notably, several works have demonstrated the existence of cellular-compartment specific T_2 values (MacKay et al., 2006). Still few studies using multi-component T_2-relaxometry have been conducted to find age-related differences in MWF, and far fewer for examining gender differences. Inconsistent findings have been, so far, reported. Specifically, two studies observed a linear increase in MWF with age (i.e., N = 27 healthy participants, age range 15–55 years (Flynn et al., 2003); and N = 44, age range 5–40 years (Lang et al., 2014)), two other studies reported a linear decrease (i.e., N = 90 healthy adults, aged 22–81 years (Papadaki et al., 2019); and N = 45, age range 18–79 years (Faizy et al., 2018)) and, yet, a couple of studies more observed mixed patterns. In the multimodal study conducted by (Billiet et al., 2015) (N = 59, age range, 17–70 years) only minor differences were found in MWF between the period of late development and early aging, with age-related positive correlations in brain regions where MWF differences were detected. Finally, another study (N = 61, age range, 18–84 years) found an inverted-U pattern of age-myelin association in six white matter tracts, with shapes differing across tracts (Arshad et al., 2016). This finding is in line with another report based on BMC-mcDESPOT, an alternative technique for quantifying MWF (Bouhrara et al., 2020).

Taken together, these results point to a poor understanding of the interaction between sex, tissue microstructure, and normal aging, and suggest the need for additional research to reveal the true direction of age-related microstructural differences and whether there is gender dimorphism. As the commonly employed neuroimaging techniques (e.g., VBM and DTI) are not specific to any tissue microstructure parameter, there exists a research gap. In our study, we aimed to quantify whole-brain voxel-based age- and sex-related differences in the largest sample of healthy adults recruited to date to perform multi-component T_2-relaxometry. The main advantage of this technique is that the information provided by the estimated T_2 spectra is more closely related to tissue microstructure parameters. Specifically, to provide a more complete and specific characterization of age- and gender-related differences, and to better interpret our findings in terms of tissue microstructure, we evaluated 5 metrics derived from the estimated T_2 spectra, including MWF, the intra- and extra-cellular water fraction, the mean T_2 relaxation time of the intra- and extra-cellular water, the total water content per voxel, and the volume fraction of the free and

quasi-free water. Notably, as these metrics are related to different portions of the spectra and quantify distinct tissue water pools, results are less affected by partial volume effects and confounding factors.

2. Methods

2.1. Sample

A total of 145 Caucasian healthy participants were recruited. The sample consisted of 91 women and 54 men with no family relationship, selected to be matched for age, estimated Intelligence Quotient (IQ), and years of education. Exclusion criteria for all participants included left-handedness, personal history of neurological disease, brain injury, presence of cardiovascular risk factors for cognitive impairment (i.e., ictus), suffering from a severe physical condition (e.g., cancer), personal or family (first degree) history of a psychiatric disorder, current or previous psychopharmacological treatment, alcohol/substance abuse/dependence in the 12 months before participation, claustrophobia, and presence of contraindications for MRI scanning (i.e. cardiac pacemaker, metal fragment/prostheses, pregnancy, surgical intervention within one month before scanning). Moreover, all participants were required to be aged between 18 and 60 years old, and to have an estimated IQ (based on the results in the Word Accentuation Test score (Test de Acentuación de Palabras (TAP) (Gomar et al., 2011), which requires pronunciation of Spanish words which have had the accents removed) in the normal range (i.e., IQ>85, TAP>14). All participants were recruited by three institutions (62 from FIDMAG Research Foundation, 46 from Universitari Institut Pere Mata, and 37 from Hospital Clínic de Barcelona, Spain), and were scanned using the same 3T MRI scanner (Philips Ingenia CX) at the Barcelonaβeta Brain Research Center, Pasqual Maragall Foundation (Barcelona, Spain). The study was carried out following the latest version of the Declaration of Helsinki, and it was reviewed by the ethical committee of the three institutions. Written informed consent was obtained from all participants.

2.2. MRI acquisition

Multi-echo T_2 data were acquired for each participant using a standard 32-channel head/neck coil and a gradient and spin-echo sequence (Prasloski et al., 2012b) with the following sequence parameters: Field-of-view = 240 × 230 mm; acquisition voxel-size = 3.5 × 3.5 mm^2, reconstructed voxel-size = 1.6 × 1.6 mm^2; number of echoes = 32; echo-time spacing (ΔTE) = 7.7 ms; repetition time (TR) = 8620 ms; excitation pulse = 90^0; refocusing pulses = 180^0; number-of-slices = 40; slice-thickness = 3.5 mm; number of averages = 1; acceleration factor (SENSE) = 2; acquisition time = 8:37 min.

2.3. Preprocessing, estimation, and spatial normalization

The brain MRI images were filtered using a 3D total variation algorithm (i.e., 'denoise_tv_chambolle' function within the 'scikit-image' python toolbox) before fitting. Spatial filtering is effective for decreasing the variability of the estimated MWF maps (Jones et al., 2003). To estimate the T_2 distribution per voxel, different dictionary matrices of synthetic signals were generated using the EPG model (Prasloski et al., 2012a), each one corresponding to a fixed refocusing flip angle value selected from a discrete set of values between 90° and 180° equally spaced by 1°. Moreover, a fixed T_2 range from 10 to 2000 ms (Prasloski et al., 2012b) with p = 60 T_2 logarithmically spaced points was employed. The fitting process was carried out independently for each matrix dictionary by using the standard non-negative least squares (NNLS) algorithm and the actual flip angle was determined as the one minimizing the mean squared error (Prasloski et al., 2012a). As the B_1 inhomogeneities are expected to be smooth and not dependent on the brain anatomy, the acquired MRI data were smoothed with a Gaussian kernel (FWMH of 4.8 mm) for determining the actual flip angle (Drenthen et al., 2019). Finally, the intra-voxel T_2 distribution was calculated by using regularized NNLS (Laule et al., 2007a; Mackay and Laule, 2012) with a second-order Laplacian regularization term to promote smooth solutions that better represent the distribution expected from tissue microstructure (Mackay et al., 1994; Whittall et al., 1997) as described in (Canales-Rodríguez et al., 2019). The regularization parameter was determined using the L-curve method (Hansen, 1992) as implemented in (Castellanos et al., 2002). The estimation was done using the multi-component T_2 reconstruction toolbox (Canales-Rodríguez et al., 2021): https://github.com/ejcanalesr/multicomponent-T2-toolbox.

From the estimated T_2 spectra, five quantitative imaging biomarkers characterizing the brain tissue were derived: (1) the total water content (TWC), proportional to the predicted signal for TE = 0 (i.e., proton density) and estimated as the area under the curve of the whole T_2 distribution (Meyers et al., 2017), (2) the MWF, calculated as the area under the curve for T_2 times smaller than the myelin water cutoff T_2=40 ms, normalized by TWC (Meyers et al., 2017), (3) the intra- and extra-cellular water fraction (IEWF), computed as the area under the T_2 distribution in the range 40−200ms, normalized by TWC, (4) the T_2 of the intra- and extracellular water (T_2^{IE}), computed as the geometric mean of the distribution in the T_2 range specified above (Bjarnason, 2011) and, (5) the water fraction of the pool with longest T_2 time, which characterizes the free and quasi-free water fraction (FQFWF) estimated as the area under the T_2 spectrum in the range 200-2000ms, normalized by TWC. Note that in previous studies this range was split into two different parts: a long-T_2 from 200−800ms and a very long-T_2 from 800−2000 ms (Laule et al., 2008, 2007b) to discriminate between the water pools present in diseased white matter and CSF (i.e., free water), respectively. In this study, we have merged both T_2 ranges and used the term 'free and quasi-free water' instead. It refers to those water molecules that do not interact with the tissue during the experimental time (i.e., free water) or that have a reduced interaction in comparison to the intra- and extra-cellular compartment (i.e., quasi-free water). On the other hand, as the estimated TWC maps are affected by spatial intensity variations due to bias field inhomogeneities (Meyers et al., 2016), they were corrected a posteriori by using the FAST v4.0 tool (Zhang et al., 2001) included in the FSL software package (for more details, see https://fsl.fmrib.ox.ac.uk/fsl/fslwiki/FAST). The underlying method is based on a hidden Markov random field model. The whole process is robust, fully automated, and produced bias field-corrected TWC images. Finally, it is important to keep in mind that the bias field correction does not affect the MWF, IEWF, and FQFWF maps, because these metrics are normalized, that is, their sum is equal to one.

After skull removal, images were normalized using the high-resolution nonlinear registration Symmetric Normalization (SyN) algorithm (Avants et al., 2008). All images were simultaneously used for coregistration, producing multimodal study-specific templates that were later applied in the final normalization. Specifically, a single deformation field was estimated for each participant by considering all the estimated metrics. Then, this field was applied to transform each image to the MNI space, as described in (Canales-Rodríguez et al., 2013). As a result, our statistical analyses are not affected by metric-specific normalization bias (i.e., miss-registration between images) because all maps from

each participant were normalized using the same deformation field. The analyses of all metrics included both GM and WM tissue, except for MWF which was restricted to WM because MWF is close to zero in the cerebral cortex. Before doing the statistical analyses, all images were spatially filtered with a Gaussian kernel of $\sigma = 2$ mm.

2.4. Statistical analyses

Differences in demographic characteristics among the groups were examined using chi-square tests (categorical variables) and ANOVAs (continuous variables).

To characterize the differential association among age, gender, and brain tissue microstructure, three statistical models were considered. The first model was designed to identify brain regions showing significant age-related differences for each gender, separately. This was done by testing for positive and negative correlations between age and each one of the five studied metrics. A second analysis was conducted to determine if the observed age-related differences were faster in one group than in another. This was done by comparing the slopes of the regression lines between males and females. Finally, a direct inter-group comparison was performed to identify the brain regions where both groups differ, after controlling for age effects. This last analysis, though, could not be performed when both groups showed different aging trajectories (i.e., second analysis) as the observed differences would be age-specific. In those cases, inter-group differences were reported at the mean age of both groups.

It is important to note that only linear relationships with age were studied because our healthy participants were aged under 60 years. Quadratic relationships (i.e. inverted U-shape patterns) between age and surrogates of myelin content have been reported in previous studies, for example, see (Bouhrara et al., 2020; Melie-Garcia et al., 2018), but these were more evident for populations involving participants over age 55–60 years. In a preliminary analysis, we plotted the variables under study and verified that their dependence with age was dominated by linear relationships, in conformity with a previous study that used the same MRI technique on participants with a similar age range (Flynn et al., 2003).

All statistical analyses were carried out by fitting voxel-wise general linear models and by applying non-parametric permutation tests, as implemented in the 'randomise' FSL tool (Jenkinson et al., 2011; Smith et al., 2004). Specifically, the Threshold-Free Cluster Enhancement (TFCE) method (Smith and Nichols, 2009) was employed using 5000 permutations. Only significant results at $p \leq 0.05$, corrected for multiple comparisons are reported. Anatomical locations of the significant white matter regions were reported considering the Johns Hopkins University (JHU) white-matter atlas (Mori et al., 2008; Oishi et al., 2008) included in FSL. Significant regions in grey matter were determined with reference to the Anatomical Automatic Labeling atlas (Tzourio-Mazoyer et al., 2002) included in the MRIcron software.

3. Results

Demographic data for the two groups of healthy controls (i.e., women and men) are shown in Table 1. Groups were matched for age, estimated IQ (TAP score), and years of education.

Fig. 1 shows average maps by age decade for each of the five studied metrics over the adult life span for one representative axial slice. Visual inspection indicates increases in MWF and FQFWF and decreases in IEWF and T_2^{IE} values with age. On the other hand, it seems that TWC remains unchanged. In the next sections, we will present results from the statistical analyses to verify if the observed trends are significant and if there are gender-related effects.

Table 1
Demographic features of the two groups of healthy participants

Variables	Women (N=91)	Men (N=54)	*p*-value
Age (years)	37.02 ± 11.24	36.48 ± 10.6	0.78
TAP	24.37 ± 3.44	24.49 ± 3.27	0.83
Years of education	15.5 ± 3.1	14.6 ± 3.5	0.13

Key: TAP, Word Accentuation Test (i.e., in Spanish: 'Test de Acentuación de Palabras').
Values are given as mean ± standard deviation.

3.1. Total water content

All analyses involving TWC were not significant. This metric did not show age-related effects, and there are no inter-group (i.e., gender) differences.

3.2. Myelin water fraction

Results for the MWF are shown in Fig. 2 and an exhaustive description of the significant clusters is reported in Table S1 of the Supplementary Material. While no regions of negative correlation between MWF and age were found, various regions showing a significant positive correlation were reported for both men and women (see panels A and B). Specifically, three clusters were detected in men and one big cluster in women, involving in both cases common white matter bundles, that is, fornix, cingulum, and inferior occipito-frontal fasciculus in the left (L) hemisphere; and the cortico-spinal tract and inferior occipito-frontal fasciculus of the right (R) hemisphere. The comparison of age-related slopes between both groups did not show significant results, suggesting that age-related MWF differences are similar in both men and women. Finally, the inter-group comparison revealed that men had higher MWF in three clusters (see Panel C and Table S1). The biggest cluster was located in the left hemisphere, spanning the corpus callosum (CC), white matter regions adjacent to the temporal middle cortex, and the posterior segment of the arcuate fasciculus. The second cluster included the uncinate fasciculus R and CC L, and the third cluster was located in the inferior longitudinal fasciculus R.

3.3. Intra- and extra-cellular water fraction

As shown in Fig. 3 (panels A and B), the IEWF decays with age in nearly all brain regions in both groups of participants, except for some white matter regions in the CC. However, this decay is more extended in men than in women (see Table S2 of the Supplementary Material). In contrast, there were no regions of significant positive correlation with age. The comparison of slopes revealed that the decay in women was milder than in men in one big cluster (see panel C) comprising several GM regions including the cuneus, angular, inferior temporal and occipital cortices, and the cerebellum in the right hemisphere, as well as the left superior occipital cortex and the medial prefrontal cortex. This cluster also reached the cingulum bundle, bilaterally. The inter-group comparison of IEWF showed that, at the average age of the pooled sample, women had a higher mean IEWF than men in three main clusters involving similar regions to those reported in the previous analysis (see panel D). However, the most significant peaks were found in different regions, that is, the inferior parietal, angular and precentral cortices in the right brain hemisphere; and the precuneus, fusiform, and inferior temporal grey matter regions on the left hemisphere.

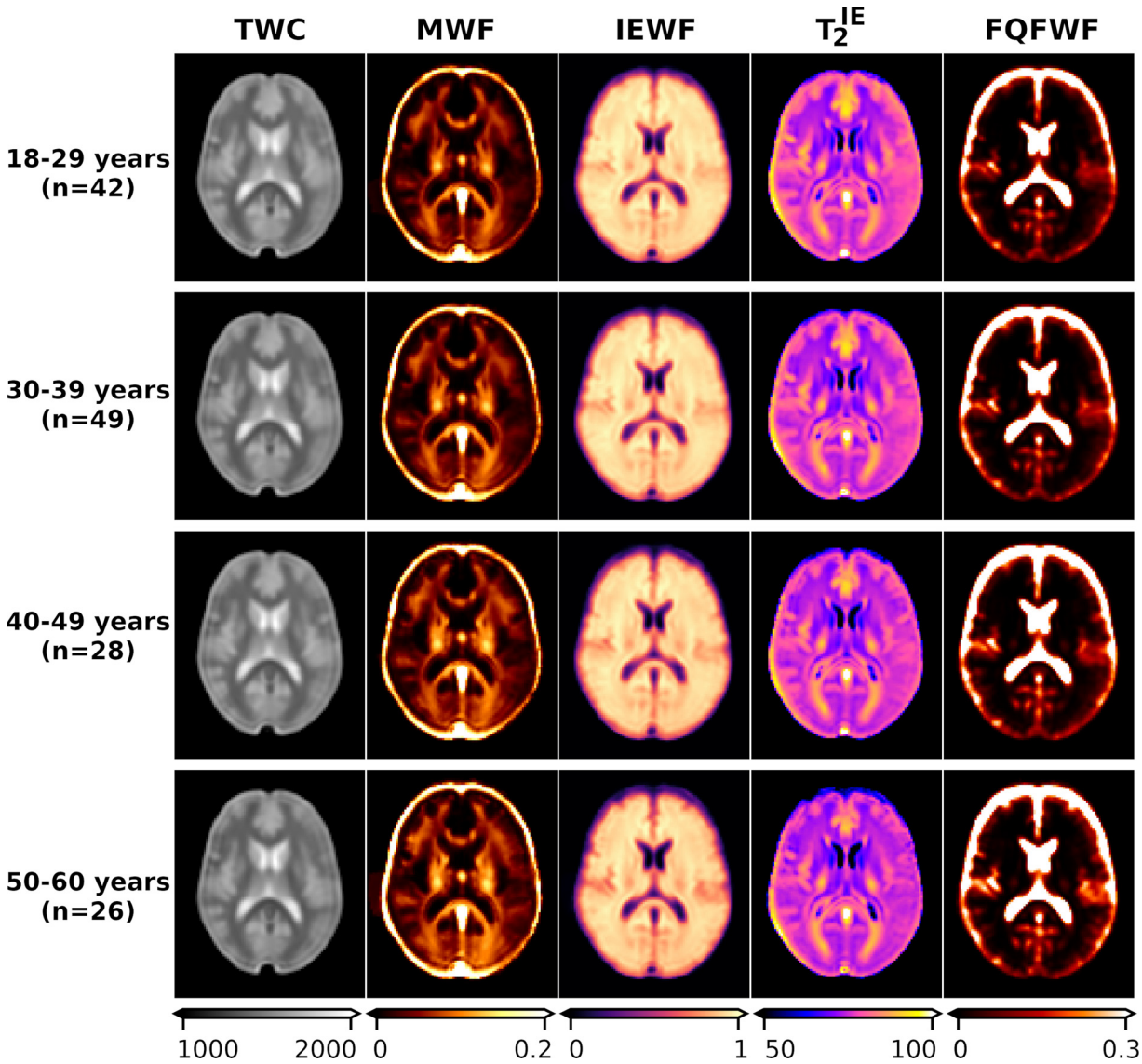

Fig. 1. Average maps from all participants in this study grouped by age decade. These maps are for illustrative purposes only. FQFWF, free and quasi-free water fraction; IEWF, intra- and extra-cellular water fraction; MWF, myelin water fraction; TWC, total water content; T_2^{IE}, T_2 relaxation time of the intra- and extra-cellular water. For interpretation of the references to color in this figure legend, the reader is referred to the Web version of this article.

3.4. Intra- and extra-cellular T_2^{IE}

The results for this metric are reported in Fig. 4 and Table S3 in Supplementary Material. Fig. 4 (panels A and B) depict brain regions where T_2^{IE} was negatively correlated with age in males and females. Although significant areas span through the whole GM, the most significant peaks were located at similar regions in both groups, that is, the temporal middle and the inferior fronto-occipital fasciculus in the left brain hemisphere; and the lingual and frontal cortices on the right side. Besides, four clusters of positive correlation were only found in the white matter of women (see panel C). The two biggest clusters were located in the CC bilaterally; the third cluster was over the left cortico-spinal tract, and the smallest cluster was found in the right inferior longitudinal fasciculus. Interestingly, no regions of positive correlation were found in men. To determine if men had a similar trend to women in these regions, we plotted (result not shown) the mean T_2^{IE} taken over these clusters versus age, and verified that the slope of the regression line was positive for men. The comparison of slopes between groups revealed that women had a significantly milder decline in several small clusters located at the anterior cingulum bilaterally, inferior and parietal cortices, left supplementary motor area, and middle temporal gyrus (see panel D and Table S3). Finally, the inter-group comparison at the mean age did not reveal any significant difference.

3.5. Free and quasi-free water fraction

No regions of negative correlation between FQFWF and age were found in any group. In contrast, significant positive correlations were found in both groups, spanning many different brain regions, see Fig. 5 (panels A and B) and Table S4 of the Supplementary Material where the most significant peaks are reported. The analysis comparing the age-related slopes revealed that men had higher slopes than women in two clusters mainly affecting the cerebral cortex but also including some white matter tracts (see panel C). The first cluster spanned across several regions and the most significant peaks were located at the precuneus, CC, and

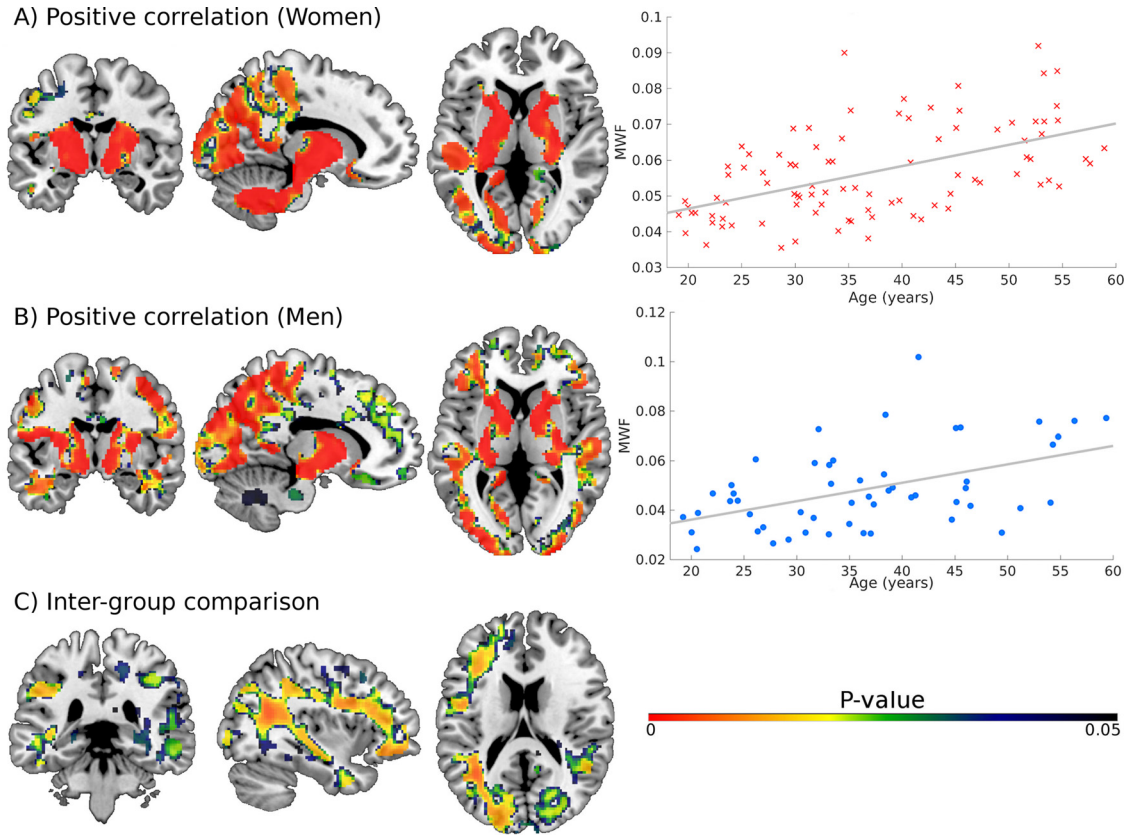

Fig. 2. Myelin water fraction (MWF) results. Panels A and B depict brain regions where MWF increases significantly with age in men and women, respectively. Scatter plots are based on the mean value over all significant voxels. Panel C shows brain regions where men have a higher MWF, after controlling for age effects. For interpretation of the references to color in this figure legend, the reader is referred to the Web version of this article.

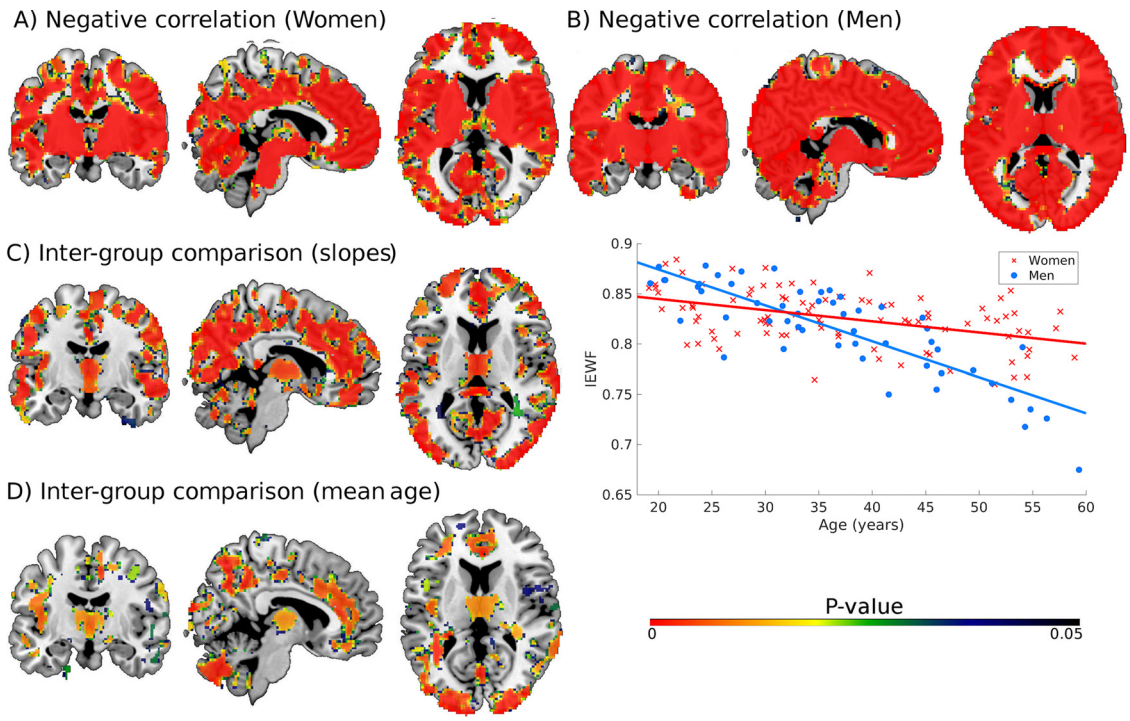

Fig. 3. Intra- and extra-cellular water fraction (IEWF) results. Panels A and B depict brain regions where IEWF decreases with age for men and women, respectively. Panel C shows brain regions where the IEWF decay is slower in women. The scatter plot shows the mean value over all the significant voxels for men and women and their corresponding regression lines. Brain regions where women had a higher IEWF at the mean age of both groups are shown in panel D. For interpretation of the references to color in this figure legend, the reader is referred to the Web version of this article.

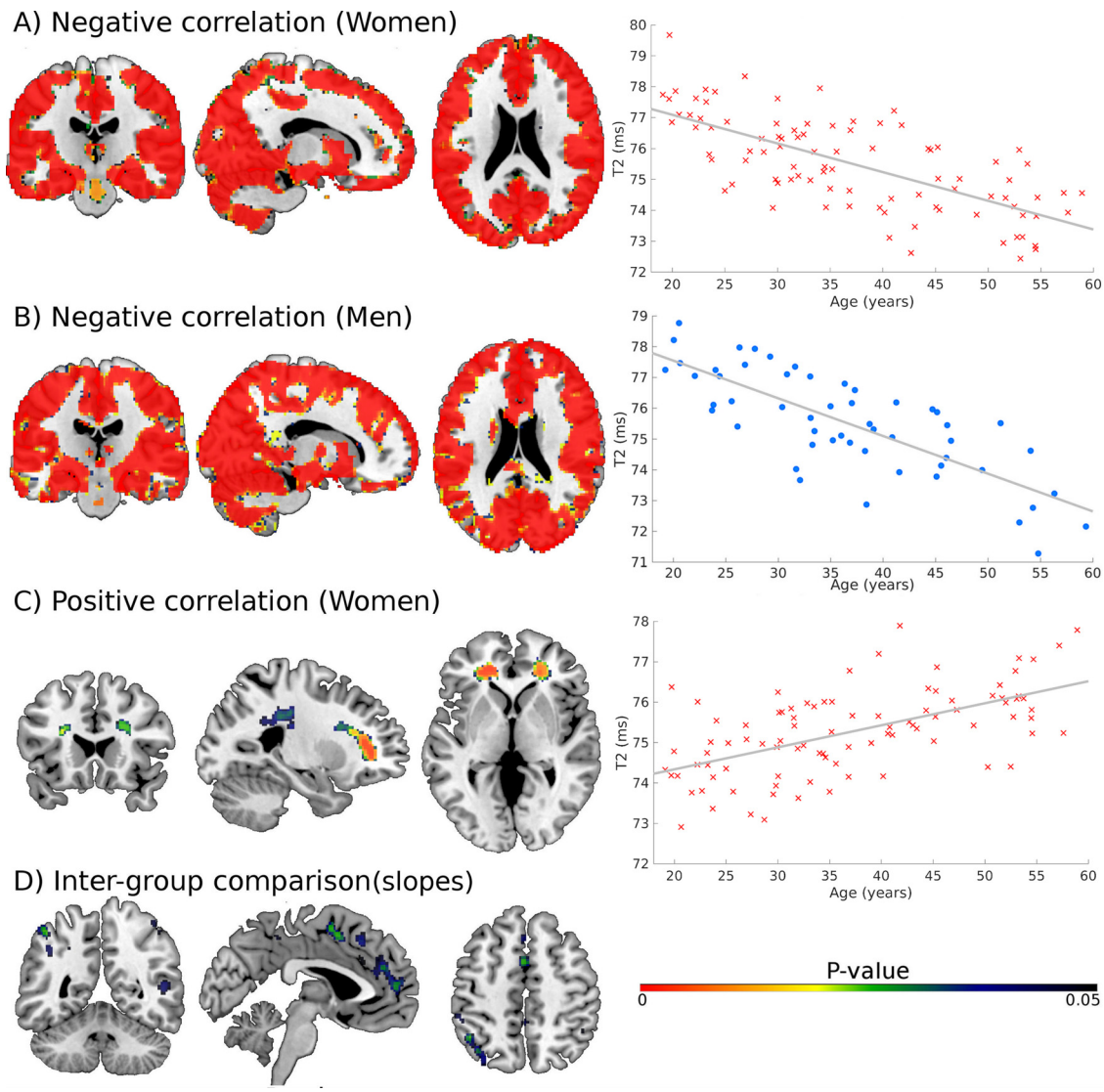

Fig. 4. Significant results in the T_2 of the intra- and extra-cellular compartment (T_2^{IE}). Panels A and B depict brain regions where T_2^{IE} decreased with age for men and women, respectively. Panel C shows brain regions where T_2^{IE} is positively correlated with age in women. The scatter plots show the mean value over all the significant voxels for all the participants and corresponding regression lines, respectively. Panel D shows brain regions where women had a higher (i.e., less negative) regression slope than men. For interpretation of the references to color in this figure legend, the reader is referred to the Web version of this article.

anterior cingulate in the left hemisphere; and the cerebellum and cingulum bundle on the right hemisphere. The second cluster was much smaller and was located in the triangular part of the inferior frontal gyrus of the left hemisphere. Finally, the inter-group comparison evaluated at the mean age of both groups showed that men had higher FQFWF than women in 8 relatively small clusters, including the cerebellum, precuneus, thalamus, lingual and the inferior longitudinal fasciculus in the left hemisphere; and the anterior part of the cingulate cortex, superior cerebellar pedunculus, and cortico-spinal tract on the right side.

4. Discussion and conclusions

Previous MRI studies support the hypothesis of age- and sex-related brain volume differences. Our results confirm that these differences also occur at the microstructure level. In the largest cross-sectional multi-component T_2 relaxometry study conducted to date, we evaluated five quantitative metrics derived from the estimated T_2 distributions. As these metrics were computed from adjacent but separated segments of the T_2 distribution, they correspond to distinct tissue compartments and, in consequence, our results are less affected by partial volume effects than previous quantitative MRI studies based on estimating the mean T_2 value per voxel.

Notably, the total water content was not affected by age or gender. This implies that the total number of water molecules per voxel is similar in men and women and that it is preserved with age. This result is in line with that reported by (Saito et al., 2012), which showed a stable proton density value in both GM and WM tissue during adulthood. Considering this finding, all of our remaining results are to be interpreted in terms of relative differences in the volume fractions and biochemical composition of the different microstructure compartments. Nevertheless, as TWC images have to be corrected for bias field inhomogeneities and different correction algorithms may produce slightly different results (Belaroussi et al., 2006), our TWC findings may depend on the chosen algorithm.

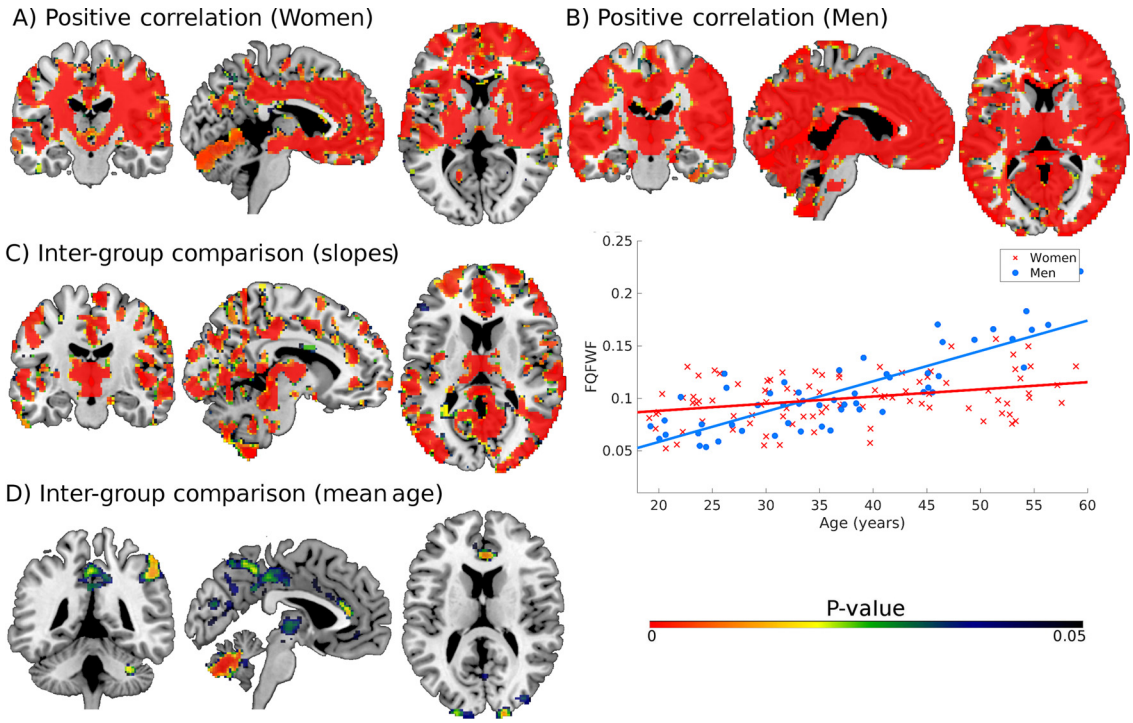

Fig. 5. Significant results in the free and quasi-free water fraction compartment. Panels A and B depict brain regions where FQFWF increases with age for both men and women groups, respectively. Panel C shows brain regions where the slope of the regression line FQFWF versus Age is higher in men. The scatter plot shows the mean value over all the significant voxels for men and women and their corresponding regression lines. Panel D depicts brain regions where men have a higher FQFWF at the mean age. For interpretation of the references to color in this figure legend, the reader is referred to the Web version of this article.

We found similar age-related MWF differences in men and women, although men exhibited a higher MWF than women in WM regions, especially in the left hemisphere. No regions with a negative correlation between MWF and age were found. In contrast, several white matter regions showed significant positive correlations for both men and women. The linear increase in MWF with age is similar to that reported in previous reports (Flynn et al., 2003; Lang et al., 2014), but is opposed to the findings in two other studies (Faizy et al., 2018; Papadaki et al., 2019). Our result is also similar to that reported in (Arshad et al., 2016); however, as our sample only included relatively young adult participants (18–60 years), we could not assess if older participants have a reduced MWF (Melie-Garcia et al., 2018). A recent study using BMC-mcDESPOT also found an inverted U-shape between age and MWF (Bouhrara et al., 2020), suggesting that myelination decreases at older ages, and especially for participants over the age of 55–60 years. Interestingly, although multi-echo T_2 relaxometry and mcDESPOT aims at computing MWF, results from both techniques have been reported to disagree, with mcDESPOT providing consistently higher estimates (Dvorak et al., 2021). Given that multi-component T_2 relaxometry is a quantitative technique, further research needs to be done regarding the acquisition sequences and reconstruction algorithms for understanding the conflicting findings across studies.

The positive correlation found between MWF and age may indicate an increase of myelin content with age in some brain regions. Although in a previous study a similar result was considered counterintuitive (Billiet et al., 2015) it may not necessarily be the case. In an outstanding review of the effects of normal aging on myelin, it was described that despite some myelin sheaths exhibit degenerative changes, myelin formation is continuing during aging (Peters, 2002). This is supported by the formation of redundant myelin and thicker sheaths (Peters, 2009), and by the fact that oligodendrocytes increase in number with age (Peters, 2002). On the other hand, multi-component T_2 analysis may not be sensitive enough to distinguish between intact myelin, degenerating myelin, and myelin debris (MacKay and Laule, 2016; Webb et al., 2003). The most common form of age-related degeneration is splitting of the myelin lamellae at the major dense line to accommodate pools of dense cytoplasm, which may decrease the axonal conduction velocity (Peters, 2002). If the T_2 associated to these pools is within the range prescribed for myelin water (i.e., 10–40 ms), then these compartments are going to inflate the actual MWF value. Unfortunately, we could not find any reference value for the T_2 of such micro-compartments.

The reported negative correlation between IEWF and age may indicate a reduction in the relative volume of the intra- and extra-axonal compartment. This result was significant throughout the whole brain, except for some regions in the corpus callosum, and was more extended in men. When we compared the regression slopes of this linear relationship we found that IEWF decays more slowly in women in one large cluster, suggesting that women may be less vulnerable to age-related changes. At the mean age for both groups, women had higher IEWF than men in regions similar to those showing different slopes. Here, it is important to recall that we are analyzing relative water fractions, which sum is normalized to unity. Therefore, the reduction in IEWF may be explained by a relative increase in MWF or FQFWF. A limitation of this technique is that we cannot separate the individual contributions from the intra- and extra-cellular compartments and only their sum can be determined. Interestingly, using the NODDI diffusion MRI model, which can separate these two terms, a linear decrease of the intra-axonal volume fraction (i.e., neurite density) with age was found in healthy participants aged 45–72 years (Merluzzi et al., 2016). This

finding was generalized to several white matter tracts in a very large population (N = 3513, age range, 45–77 years) from the UK Biobank (Cox et al., 2016).

Our results revealed a strong negative correlation between T_2^{IE} and age extending through the whole grey matter and reaching a few white matter tracts in both groups. Notably, a significant positive correlation was found in women but not in men in the frontal WM and when we compared the regression slopes, we found that the T_2^{IE} decay was slower in women in various small clusters. On the other hand, the inter-group comparison at the mean age for both groups did not show any significant difference. Interpreting these results in terms of tissue microstructure is challenging because T_2 depends on a number of factors. For instance, it is well known that it depends on the surface-to-volume (SA:V) ratio and the surface relaxivity of the sample (Brownstein and Tarr, 1979; Cohen and Mendelson, 1982). Considering this evidence, the observed increase in T_2 in some white matter regions may be explained by a smaller SA:V ratio caused by a reduction in the neurite density, or by a reduction in the surface relaxivity of the cells. Moreover, the T_2 reduction in GM regions may be partially explained by an age-related increase in the number of macromolecules, iron deposition (Correia et al., 2010), dysregulation of neuronal Ca^{2+} homeostasis, and accumulation of dysfunctional and aggregated proteins as a result of oxidative imbalance (Mattson and Arumugam, 2018), which distorts the uniformity of the local magnetic field experienced by the hydrogen protons.

Finally, FQFWF results involved extended positive correlations with age in both genders, but faster increases in men, mainly affecting the GM tissue and some WM tracts. Results from the inter-group comparison at the mean age revealed several small regions where on average men had higher FQFWF than women (in both GM and WM tissue). We are not the first group reporting a positive correlation between FQFWF and age. An earlier optimized VBM study showed a significant increase in the free water compartment (i.e., CSF) obtained after segmenting T1w images from 465 adult brains (Good et al., 2001). This result has been also replicated in more recent VBM studies (Smith et al., 2007) and by analyses using multi-shell diffusion MRI data (Cox et al., 2016; Merluzzi et al., 2016). This result suggests that men may be more susceptible to aging effects.

Our results revealed a sexual dimorphism in the brain tissue microstructure, with WM areas showing increased MWF and GM areas showing increased FQFWF and decreased T_2^{IE} in men, respectively. While sexual dimorphism has been well described by several volumetric MRI studies, for example, see (Coffey et al., 1998; Gur et al., 1991; Leonard et al., 2008), only a few studies have investigated gender differences in brain microstructure. And most of these, either employed nonspecific metrics from DTI, for example, (Bava et al., 2011; Kanaan et al., 2012; Liu et al., 2010; Westerhausen et al., 2003) or used more specific techniques (e.g., multi-echo T_2 relaxometry) in small samples (Faizy et al., 2018; Liu et al., 2010). Other multi-echo T_2 relaxometry studies with relatively larger samples did not investigate gender effects, for example, (Billiet et al., 2015; Flynn et al., 2003; Lang et al., 2014). Interestingly, our findings might be in line with previous evolutionary theories suggesting that males and females age at different rates, resulting in longevity gender gaps (Barrett and Richardson, 2011; Blagosklonny, 2010; Regan and Partridge, 2013). Although it has been suggested by different groups that sexual differentiation of the human brain is a multi-factorial process as a consequence of the influence of genetic factors and sex hormones on brain organization during development (Zaidi, 2010) (which also exists in most sexually reproducing species (Regan and Partridge, 2013)), a comprehensive explanation for understanding the underlying mechanisms at the cellular level does not exist yet. Consequently, we cannot explain how this multi-factorial process shapes the brain tissues and the water pools measured in our study. Our work adds more evidence supporting a sexual dimorphism at the microstructural level, complementing previous volumetric and functional MRI studies (Koch et al., 2007; Salvador et al., 2020).

We have used an experimental repetition time (i.e., TR = 8620 ms) higher than those used in previous studies (i.e., TR range, 1100 – 3800ms). This may be an important advantage, as this implies that our measured signals are less affected by T_1 effects. If the signal depends on the T_1 relaxation time, a change in T_1 with age may be wrongly interpreted as a relative water fraction change. And in fact, previous studies have shown T_1 variations with age (Okubo et al., 2017; Yeatman et al., 2014). Other methodological advantages of our study can be mentioned. First, the data were acquired in a modern 3T scanner, while some previous studies used 1.5T (Flynn et al., 2003; Lang et al., 2014; Papadaki et al., 2019). Moreover, the acquisition spanned the whole brain, whereas some of the previous studies only acquired a few slices with very large slice-thickness (i.e., 8 – 10 mm) (Flynn et al., 2003; Lang et al., 2014; Papadaki et al., 2019), thus our analysis is less affected by localization errors across participants. Additionally, we performed voxelwise whole-brain analyses while previous studies evaluated a few preselected regions of interest. Finally, in contrast to previous studies that mainly focused on MWF, here we also evaluated other four imaging biomarkers computed from the T_2 spectra, including the total water content, the intra- and extra-cellular water fraction and its corresponding T_2, and the free and quasi-free water fraction.

While our work is the largest multi-component T_2 relaxometry study conducted to date in healthy adults, certain limitations remain. Even if our cohort included a wide age range, it did not include very young (<18 years) and very old (>60 years) participants and thus our findings cannot be extrapolated outside the studied age range. Also, although both genders were matched by age, and age was added as a covariate in the statistical analyses, we still had more females (N = 91) than males (N = 54). Consequently, the parameters estimated (e.g., slope and intercept) for the women group were probably more robust (i.e. they had less variance and more statistical power to detect significant patterns). This was not a problem for between gender comparisons but may have potentially led to less extended patterns in analyses involving only males. Yet, in our opinion, the number of participants in the men's group was large enough to achieve accurate results and to uncover major male-related traits, as is strongly suggested by the large extent of male-related clusters shown in Figs. 2–5.

A further concern is that the employed methodology does not account for additional confounding factors that may modulate the measured signals, such as iron deposition (Birkl et al., 2019) and magnetization transfer effects (Malik et al., 2018), which could compromise the validity of our results. Moreover, the employed technique might not be sensitive enough to distinguish between intact myelin, degenerating myelin, and myelin debris. Although using a 3T field strength is in general advantageous over a 1.5T, it produces stronger field inhomogeneities and introduces new challenges for correcting the TWC map. Future developments need to be implemented to properly model these factors and to further minimize partial volume effects by using acquisition sequences with a higher spatial resolution (Piredda et al., 2021). The MRI sequence used in this work was designed for studying healthy participants without brain lesions. Future studies focused on brain diseases may opt for using an increased data acquisition window, that is, a longer TE range (Dvorak et al., 2020) for improving the detection of tissue components with long-T_2 (Kumar et al., 2018), as those previously reported in Multiple Sclerosis and Phenylketonuria, and the posterior internal capsules of healthy

participants (Laule et al., 2007b). It is important to note that the correlation analyses conducted in this study do not imply a causal relationship and that other variables partially related to age may have influenced the results. However, there were no gender differences in any of the collected demographic variables. In a secondary analysis, we repeated the statistical tests after including estimated IQ as a covariate, and the same findings were obtained (result not shown). Additionally, we repeated the analyses by using an alternative T_2 spectrum estimation technique (Guo et al., 2013), and all of our results remained valid (result not shown). Nevertheless, other promising reconstruction techniques could be explored, including multi-voxel spatial regularized algorithms (Kumar et al., 2018) and machine learning (Yu et al., 2021). Finally, we have not evaluated the relationship between brain tissue microstructure and age-related cognitive decline.

In summary, using advanced multi-component T_2 relaxometry in a large population of healthy adults we have found age- and gender-related differences in brain tissue microstructure. Our results revealed similar age-related MWF differences in men and women; increased MWF content in men (in a few WM tracts); a faster decline with age of IEWF and T_2^{IE} in men (the negative slopes of the regression lines were steeper); and a faster increase in FQFWF in men (spanning the whole GM). By visually inspecting the regression slopes of the studied metrics, it seems that on average, women's brains may be less vulnerable to age changes than those from men from 35 – 40 years onwards. Future longitudinal studies should be conducted to confirm our findings, and to investigate if these results could explain the less age-associated cognitive decline observed in women (Gur and Gur, 2002; McCarrey et al., 2016). The strong association between the evaluated parameters and age suggests that these could be used as sensitive imaging biomarkers to reveal insight into the aging mechanism. However, from the methodological point of view, new developments are required to improve the specificity of this technique. These should be oriented to minimize the impact of confounding factors like iron deposition and magnetization transfer effects, to increase the spatial resolution of the acquired data, and to separate the intra- and extra-cellular compartments by complementing T_2 relaxometry with advanced diffusion MRI models, for example, (Barakovic et al., 2021). This report provides valuable normative data for future studies using this technique.

Disclosure statement

Dr. Vieta has received grants and served as consultant, advisor, or CME speaker for the following entities (unrelated to the present work): AB-Biotics, Abbott, Allergan, Angelini, Dainippon Sumitomo Pharma, Ferrer, Gedeon Richter, Janssen, Lundbeck, Otsuka, Sage, Sanofi-Aventis, and Takeda. The other authors have nothing to disclose.

Author Contributions

Erick Jorge Canales-Rodríguez: Conceptualization, Data curation, Formal analysis, Funding acquisition, Investigation, Methodology, Project administration, Resources, Software, Visualization, Roles/Writing - original draft, Writing - review & editing. **Silvia Alonso-Lana:** Data curation, Investigation, Writing - review & editing. **Norma Verdolini:** Data curation, Investigation, Writing - review & editing. **Salvador Sarró:** Data curation, Investigation, Writing - review & editing. **Isabel Feria:** Data curation, Investigation, Writing - review & editing. **Irene Montoro:** Data curation, Investigation, Writing - review & editing. **Beatriz Garcia-Ruiz:** Data curation, Investigation, Writing - review & editing. **Esther Jimenez:** Data curation, Investigation, Writing - review & editing. **Cristina Varo:** Data curation, Investigation, Writing - review & editing. **Auria Albacete:** Data curation, Investigation, Writing - review & editing. **Isabel Argila-Plaza:** Data curation, Investigation, Writing - review & editing. **Anna Lluch:** Data curation, Investigation, Writing - review & editing. **Caterina del Mar Bonnin:** Data curation, Investigation, Writing - review & editing. **Elisabet Vilella:** Data curation, Funding acquisition, Investigation, Project administration, Resources, Writing - review & editing. **Eduard Vieta:** Data curation, Funding acquisition, Investigation, Project administration, Resources, Writing - review & editing. **Edith Pomarol-Clotet:** Conceptualization, Data curation, Funding acquisition, Investigation, Project administration, Resources, Supervision, Writing - review & editing. **Raymond Salvador:** Conceptualization, Funding acquisition, Investigation, Methodology, Validation, Writing - review & editing.

Acknowledgements

This work was supported by the Generalitat de Catalunya: 2014SGR1573, 2014SGR398 and 2017SGR1365 and by the Centro de Investigación Biomédica en Red de Salud (CIBERSAM). Also by several grants funded by the Instituto de Salud Carlos III and the Spanish Ministry of Science, Innovation, and Universities (co-funded by the European Regional Development Fund/European Social Fund "Investing in your future"): Sara Borrell Research Contract (CD18/00029 to EC-R and CD19/00232 to SA-L), Río Hortega (CM17/00258 to NV), Miguel Servet Research Contract (CPII16/00018 to EP-C and CPII13/00018 to RS), Research Mobility programme (MV18/00054 to EP-C), Research Projects (PI15/00277 to EC-R, PI15/00852 and PI18-00945 to EV, PI15/00283 and PI18/00805 to EV, PI14/01151 to RS, PI14/01148 and PI18/00810 to EP-C). -. EC-R was also supported by the Swiss National Science Foundation, Ambizione grant PZ00P2_185814. The funding organizations played no role in the study design, data collection, analysis, or manuscript approval. We finally thank all the study participants.

Supplementary materials

Supplementary material associated with this article can be found, in the online version, at doi:10.1016/j.neurobiolaging.2021.06.002.

References

Alonso-Ortiz, E., Levesque, I.R., Pike, G.B., 2015. MRI-based myelin water imaging: a technical review. Magn. Reson. Med. 73, 70–81. doi:10.1002/mrm.25198.

Arshad, M., Stanley, J.A., Raz, N., 2016. Adult age differences in subcortical myelin content are consistent with protracted myelination and unrelated to diffusion tensor imaging indices. Neuroimage. 143, 26–39. doi:10.1016/j.neuroimage.2016.08.047.

Ashburner, J., Friston, K.J., 2000. Voxel-based morphometry–the methods. Neuroimage. 11, 805–821. doi:10.1006/nimg.2000.0582S1053-8119(00)90582-2, [pii].

Avants, B.B., Epstein, C.L., Grossman, M., Gee, J.C., 2008. Symmetric diffeomorphic image registration with cross-correlation: evaluating automated labeling of elderly and neurodegenerative brain. Med. Image. Anal. 12, 26–41. doi:10.1016/j.media.2007.06.004, doi:S1361-8415(07)00060-6 [pii].

Barakovic, M., Tax, C.M.W., Rudrapatna, U., Chamberland, M., Rafael-Patino, J., Granziera, C., Thiran, J.P., Daducci, A., Canales-Rodríguez, E.J., Jones, D.K., 2021. Resolving bundle-specific intra-axonal T2 values within a voxel using diffusion-relaxation tract-based estimation. Neuroimage. 227, 117617. doi:10.1016/j.neuroimage.2020.117617.

Barrett, E.L.B., Richardson, D.S., 2011. Sex differences in telomeres and lifespan. Aging. Cell doi:10.1111/j.1474-9726.2011.00741.x.

Basser, P.J., Mattiello, J., LeBihan, D., 1994. Estimation of the effective self-diffusion tensor from the NMR spin echo. J. Magn. Reson .B. 103, 247–254.

Bava, S., Boucquey, V., Goldenberg, D., Thayer, R.E., Ward, M., Jacobus, J., Tapert, S.F., 2011. Sex differences in adolescent white matter architecture. Brain. Res doi:10.1016/j.brainres.2010.12.051.

Beaulieu, C., 2002. The basis of anisotropic water diffusion in the nervous system - a technical review. NMR. Biomed. 15, 435–455. doi:10.1002/nbm.782.

Belaroussi, B., Milles, J., Carme, S., Zhu, Y.M., Benoit-Cattin, H., 2006. Intensity non-uniformity correction in MRI: existing methods and their validation. Med. Image Anal. 10, 234–246. doi:10.1016/j.media.2005.09.004.

Berman, S., West, K.L., Does, M.D., Yeatman, J.D., Mezer, A.A., 2018. Evaluating g-ratio weighted changes in the corpus callosum as a function of age and sex. Neuroimage doi:10.1016/j.neuroimage.2017.06.076.

Billiet, T., Vandenbulcke, M., M??dler, B., Peeters, R., Dhollander, T., Zhang, H., Deprez, S., Van den Bergh, B.R.H.H., Sunaert, S., Emsell, L., Mädler, B., Peeters, R., Dhollander, T., Zhang, H., Deprez, S., Van den Bergh, B.R.H.H., Sunaert, S., Emsell, L., 2015. Age-related microstructural differences quantified using myelin water imaging and advanced diffusion MRI. Neurobiol. Aging. 36, 2107–2121. doi:10.1016/j.neurobiolaging.2015.02.029.

Birkl, C., Birkl-Toeglhofer, A.M., Endmayr, V., Höftberger, R., Kasprian, G., Krebs, C., Haybaeck, J., Rauscher, A., 2019. The influence of brain iron on myelin water imaging. Neuroimage. 199, 545–552. doi:10.1016/j.neuroimage.2019.05.042.

Bjarnason, T.A., 2011. Proof that gmT2 is the reciprocal of gmR2. Concepts Magn. Reson. Part A 38A, 128–131. doi:10.1002/cmr.a.20216.

Blagosklonny, M.V., 2010. Why men age faster but reproduce longer than women: MTOR and evolutionary perspectives. Aging (Albany. NY). 2, 265–273. doi:10.18632/aging.100149.

Bouhrara, M., Rejimon, A.C., Cortina, L.E., Khattar, N., Bergeron, C.M., Ferrucci, L., Resnick, S.M., Spencer, R.G., 2020. Adult brain aging investigated using BMC-mcDESPOT–based myelin water fraction imaging. Neurobiol. Aging. 85, 131–139. doi:10.1016/j.neurobiolaging.2019.10.003.

Brownstein, K.R., Tarr, C.E., 1979. Importance of classical diffusion in NMR studies of water in biological cells. Phys. Rev. A 19, 2446–2453. doi:10.1103/PhysRevA.19.2446.

Canales-Rodríguez, E.J., Pizzolato, M., Piredda, Gian Franco, Hilbert, T., Kunz, N., Kober, T., Thiran, J.-P., Pot, C., Daducci, A., 2019. Robust myelin water imaging from multi-echo T2 data using second-order Tikhonov regularization with control points. ISMRM 27th Annual Meeting & Exhibition, 11-16 May 2019. Montréal, QC, Canada. Montreal, Canada p. ID: 4686.

Canales-Rodríguez, E.J., Pizzolato, M., Piredda, G.F., Hilbert, T., Kunz, N., Pot, C., Yu, T., Salvador, R., Pomarol-Clotet, E., Kober, T., Thiran, J.-P., Daducci, A., 2021. Comparison of non-parametric T2 relaxometry methods for myelin water quantification. Med. Image Anal., 101959 doi:10.1016/j.media.2021.101959.

Canales-Rodríguez, E.J., Pomarol-Clotet, E., Radua, J., Sarró, S., Alonso-Lana, S., Del Mar Bonnín, C., Goikolea, J.M., Maristany, T., García-Álvarez, R., Vieta, E., McKenna, P., Salvador, R., 2013. Structural abnormalities in bipolar euthymia: a multicontrast molecular diffusion imaging study. Biol. Psychiatry. 76, 239–248. doi:10.1016/j.biopsych.2013.09.027.

Castellanos, J.L., Gómez, S., Guerra, V., 2002. The triangle method for finding the corner of the L-curve. Appl. Numer. Math. doi:10.1016/S0168-9274(01)00179-9.

Coffey, C.E., Lucke, J.F., Saxton, J.A., Ratcliff, G., Unitas, L.J., Billig, B., Bryan, R.N., 1998. Sex differences in brain aging: a quantitative magnetic resonance imaging study. Arch. Neurol. 55, 169–179. doi:10.1001/archneur.55.2.169.

Cohen, M.H., Mendelson, K.S., 1982. Nuclear magnetic relaxation and the internal geometry of sedimentary rocks. J. Appl. Phys. doi:10.1063/1.330526.

Correia, S., Hubbard, E., Hassenstab, J., Yip, A., Vymazal, J., Herynek, V., Giedd, J., Murphy, D.L., Greenberg, B.D., 2010. Basal Ganglia MR relaxometry in obsessive-compulsive disorder: T2 depends upon age of symptom onset. Brain. Imaging. Behav 4, 35–45. doi:10.1007/s11682-009-9083-2.

Cox, S.R., Ritchie, S.J., Tucker-Drob, E.M., Liewald, D.C., Hagenaars, S.P., Davies, G., Wardlaw, J.M., Gale, C.R., Bastin, M.E., Deary, I.J., 2016. Ageing and brain white matter structure in 3,513 UK Biobank participants. Nat. Commun. 7. doi:10.1038/ncomms13629.

Drenthen, G.S., Backes, W.H., Aldenkamp, A.P., Jansen, J.F.A., 2019. Applicability and reproducibility of 2D multi-slice GRASE myelin water fraction with varying acquisition acceleration. Neuroimage. 195, 333–339. doi:10.1016/j.neuroimage.2019.04.011.

Dunst, B., Benedek, M., Koschutnig, K., Jauk, E., Neubauer, A.C., 2014. Sex differences in the IQ-white matter microstructure relationship: a DTI study. Brain. Cogn 91, 71–78. doi:10.1016/j.bandc.2014.08.006.

Dvorak, A.V., Ljungberg, E., Vavasour, I.M., Lee, L.E., Abel, S., Li, D.K.B., Traboulsee, A., MacKay, A.L., Kolind, S.H., 2021. Comparison of multi echo T2 relaxation and steady state approaches for myelin imaging in the central nervous system. Sci. Rep. 11, 1369. doi:10.1038/s41598-020-80585-7.

Dvorak, A.V., Wiggermann, V., Gilbert, G., Vavasour, I.M., MacMillan, E.L., Barlow, L., Wiley, N., Kozlowski, P., MacKay, A.L., Rauscher, A., Kolind, S.H., 2020. Multi-spin echo T2 relaxation imaging with compressed sensing (METRICS) for rapid myelin water imaging. Magn. Reson. Med. 84, 1264–1279. doi:10.1002/mrm.28199.

Faizy, T.D., Kumar, D., Broocks, G., Thaler, C., Flottmann, F., Leischner, H., Kutzner, D., Hewera, S., Dotzauer, D., Stellmann, J.P., Reddy, R., Fiehler, J., Sedlacik, J., Gellißen, S., 2018. Age-related measurements of the myelin water fraction derived from 3D multi-echo GRASE reflect myelin content of the cerebral white matter. Sci. Rep. 8, 14991. doi:10.1038/s41598-018-33112-8.

Flynn, S.W., Lang, D.J., Mackay, A.L., Goghari, V., Vavasour, I.M., Whittall, K.P., Smith, G.N., Arango, V., Mann, J.J., Dwork, A.J., Falkai, P., Honer, W.G., 2003. Abnormalities of myelination in schizophrenia detected in vivo with MRI, and post-mortem with analysis of oligodendrocyte proteins. Mol. Psychiatry 8, 811–820. doi:10.1038/sj.mp.4001337.

Gennatas, E.D., Avants, B.B., Wolf, D.H., Satterthwaite, T.D., Ruparel, K., Ciric, R., Hakonarson, H., Gur, R.C.R.E., Gur, R.C.R.E., 2017. Age-related effects and sex differences in gray matter density, volume, mass, and cortical thickness from childhood to young adulthood. J. Neurosci. 37, 5065–5073. doi:10.1523/JNEUROSCI.3550-16.2017.

Gomar, J.J., Ortiz-Gil, J., McKenna, P.J., Salvador, R., Sans-Sansa, B., Sarro, S., Guerrero, A., Pomarol-Clotet, E., 2011. Validation of the Word Accentuation Test (TAP) as a means of estimating premorbid IQ in Spanish speakers. Schizophr Res 128, 175–176. doi:10.1016/j.schres.2010.11.016S0920-9964(10)01645-2, [pii].

Good, C.D., Johnsrude, I.S., Ashburner, J., Henson, R.N., Friston, K.J., Frackowiak, R.S., 2001. A voxel-based morphometric study of ageing in 465 normal adult human brains. Neuroimage 14, 21–36. doi:10.1006/nimg.2001.0786, doi:S1053-8119(01)90786-4 [pii].

Guo, J., Ji, Q., Reddick, W.E., 2013. Multi-slice myelin water imaging for practical clinical applications at 3.0 T. Magn. Reson. Med. doi:10.1002/mrm.24527.

Gur, R.C., Mozley, P.D., Resnick, S.M., Gottlieb, G.L., Kohn, M., Zimmerman, R., Herman, G., Atlas, S., Grossman, R., Berretta, D., Erwin, R., Gur, R.E., 1991. Gender differences in age effect on brain atrophy measured by magnetic resonance imaging. Proc. Natl. Acad. Sci. U. S. A. 88, 2845–2849. doi:10.1073/pnas.88.7.2845.

Gur, R.E., Gur, R.C., 2002. Gender differences in aging: Cognition, emotions, and neuroimaging studies. Dialogues Clin. Neurosci. 4, 197–210.

Hansen, P.C., 1992. Analysis of Discrete Ill-Posed Problems by Means of the L-Curve. SIAM Rev doi:10.1137/1034115.

Jenkinson, M., Beckmann, C.F., Behrens, T.E., Woolrich, M.W., Smith, S.M., 2011. Fsl. Neuroimage doi:10.1016/j.neuroimage.2011.09.015, doi:S1053-8119(11)01060-3 [pii].

Jones, C.C.K., Whittall, K.P.K., MacKay, A.L., 2003. Robust myelin water quantification: averaging versus spatial filtering. Magn. Reson. Med. 50. doi:10.1002/mrm.10492.

Jones, D.K., Cercignani, M., 2010. Twenty-five pitfalls in the analysis of diffusion MRI data. NMR Biomed doi:10.1002/nbm.1543.

Kanaan, R.A., Allin, M., Picchioni, M., Barker, G.J., Daly, E., Shergill, S.S., Woolley, J., McGuire, P.K., 2012. Gender differences in white matter microstructure. PLoS One 7. doi:10.1371/journal.pone.0038272.

Koch, K., Pauly, K., Kellermann, T., Seiferth, N.Y., Reske, M., Backes, V., Stöcker, T., Shah, N.J., Amunts, K., Kircher, T., Schneider, F., Habel, U., 2007. Gender differences in the cognitive control of emotion: an fMRI study. Neuropsychologia. 45, 2744–2754. doi:10.1016/j.neuropsychologia.2007.04.012.

Kumar, D., Hariharan, H., Faizy, T.D., Borchert, P., Siemonsen, S., Fiehler, J., Reddy, R., Sedlacik, J., 2018. Using 3D spatial correlations to improve the noise robustness of multi component analysis of 3D multi echo quantitative T2 relaxometry data. Neuroimage. 178, 583–601. doi:10.1016/j.neuroimage.2018.05.026.

Lang, D.J.M., Yip, E., Mackay, A.L., Thornton, A.E., Vila-Rodriguez, F., Macewan, G.W., Kopala, L.C., Smith, G.N., Laule, C., Macrae, C.B., Honer, W.G., 2014. 48 echo T2 myelin imaging of white matter in first-episode schizophrenia: evidence for aberrant myelination. NeuroImage Clin 6, 408–414. doi:10.1016/j.nicl.2014.10.006.

Laule, C., Kozlowski, P., Leung, E., Li, D.K.B., MacKay, A.L., Moore, G.R.W., 2008. Myelin water imaging of multiple sclerosis at 7 T: correlations with histopathology. Neuroimage 40, 1575–1580. doi:10.1016/j.neuroimage.2007.12.008.

Laule, C., Vavasour, I.M., Kolind, S.H., Li, D.K.B.B., Traboulsee, T.L., Moore, G.R.W.W., MacKay, A.L., 2007a. Magnetic resonance imaging of myelin. Neurotherapeutics. 4, 460–484. doi:10.1016/j.nurt.2007.05.004.

Laule, C., Vavasour, I.M., Mädler, B., Kolind, S.H., Sirrs, S.M., Brief, E.E., Traboulsee, A.L., Moore, G.R.W., Li, D.K.B., MacKay, A.L., 2007b. MR evidence of long T2 water in pathological white matter. J. Magn. Reson. Imaging 26, 1117–1121. doi:10.1002/jmri.21132.

Leonard, C.M., Towler, S., Welcome, S., Halderman, L.K., Otto, R., Eckert, M.A., Chiarello, C., 2008. Size matters: cerebral volume influences sex differences in neuroanatomy. Cereb. Cortex. doi:10.1093/cercor/bhn052.

Liu, F., Vidarsson, L., Winter, J.D., Tran, H., Kassner, A., 2010. Sex differences in the human corpus callosum microstructure: a combined T2 myelin-water and diffusion tensor magnetic resonance imaging study. Brain. Res. 1343, 37–45. doi:10.1016/j.brainres.2010.04.064S0006-8993(10)00981-9, [pii].

Mackay, A., Laule, C., 2012. Myelin water imaging, in: EMagRes. pp. 605–616. doi:10.1002/9780470034590.emrstm1270

MacKay, A., Laule, C., Vavasour, I., Bjarnason, T., Kolind, S., Mädler, B., 2006. Insights into brain microstructure from the T2 distribution. Magn. Reson. Imaging. doi:10.1016/j.mri.2005.12.037.

Mackay, A., Whittall, K., Adler, J., Li, D., Paty, D., Graeb, D., 1994. In vivo visualization of myelin water in brain by magnetic resonance. Magn. Reson. Med. 31, 673–677. doi:10.1002/mrm.1910310614.

MacKay, A.L., Laule, C., 2016. Magnetic resonance of myelin water: an in vivo marker for myelin. Brain Plast 2, 71–91. doi:10.3233/BPL-160033.

Malik, S.J., Teixeira, R.P.A.G., Hajnal, J.V., 2018. Extended phase graph formalism for systems with magnetization transfer and exchange. Magn. Reson. Med. 80, 767–779. doi:10.1002/mrm.27040.

Mattson, M.P., Arumugam, T.V., 2018. Hallmarks of brain aging: adaptive and pathological modification by metabolic states. Cell Metab doi:10.1016/j.cmet.2018.05.011.

McCarrey, A.C., An, Y., Kitner-Triolo, M.H., Ferrucci, L., Resnick, S.M., 2016. Sex differences in cognitive trajectories in clinically normal older adults. Psychol. Aging 31, 166–175. doi:10.1037/pag0000070.

Mechelli, A., Price, C., Friston, K., Ashburner, J., 2005. Voxel-Based Morphometry of the Human Brain: Methods and Applications Current Me.

Melie-Garcia, L., Slater, D., Ruef, A., Sanabria-Diaz, G., Preisig, M., Kherif, F., Dragan-

ski, B., Lutti, A., 2018. Networks of myelin covariance. Hum. Brain Mapp. 39, 1532–1554. doi:10.1002/hbm.23929.
Merluzzi, A.P., Dean, D.C., Adluru, N., Suryawanshi, G.S., Okonkwo, O.C., Oh, J.M., Hermann, B.P., Sager, M.A., Asthana, S., Zhang, H., Johnson, S.C., Alexander, A.L., Bendlin, B.B., 2016. Age-dependent differences in brain tissue microstructure assessed with neurite orientation dispersion and density imaging. Neurobiol. Aging. doi:10.1016/j.neurobiolaging.2016.03.026.
Meyers, S.M., Kolind, S.H., Laule, C., MacKay, A.L., 2016. Measuring water content using T2 relaxation at 3 T: phantom validations and simulations. Magn. Reson. Imaging 34, 246–251. doi:10.1016/j.mri.2015.11.008.
Meyers, S.M., Kolind, S.H., MacKay, A.L., 2017. Simultaneous measurement of total water content and myelin water fraction in brain at 3 T using a T2 relaxation based method. Magn. Reson. Imaging 37, 187–194. doi:10.1016/j.mri.2016.12.001.
Mori, S., Oishi, K., Jiang, H., Jiang, L., Li, X., Akhter, K., Hua, K., Faria, A.V., Mahmood, A., Woods, R., Toga, A.W., Pike, G.B., Neto, P.R., Evans, A., Zhang, J., Huang, H., Miller, M.I., van Zijl, P., Mazziotta, J., 2008. Stereotaxic white matter atlas based on diffusion tensor imaging in an ICBM template. Neuroimage doi:10.1016/j.neuroimage.2007.12.035.
Oishi, K., Zilles, K., Amunts, K., Faria, A., Jiang, H., Li, X., Akhter, K., Hua, K., Woods, R., Toga, A.W., Pike, G.B., Rosa-Neto, P., Evans, A., Zhang, J., Huang, H., Miller, M.I., van Zijl, P.C.M., Mazziotta, J., Mori, S., 2008. Human brain white matter atlas: Identification and assignment of common anatomical structures in superficial white matter. Neuroimage doi:10.1016/j.neuroimage.2008.07.009.
Okubo, G., Okada, Tomohisa, Yamamoto, A., Fushimi, Y., Okada, Tsutomu, Murata, K., Togashi, K., 2017. Relationship between aging and T1 relaxation time in deep gray matter: A voxel-based analysis. J. Magn. Reson. Imaging 46, 724–731. doi:10.1002/jmri.25590.
Papadaki, E., Kavroulakis, E., Kalaitzakis, G., Karageorgou, D., Makrakis, D., Maris, T.G., Simos, P.G., 2019. Age-related deep white matter changes in myelin and water content: A T2 relaxometry study. J. Magn. Reson. Imaging 50, 1393–1404. doi:10.1002/jmri.26707.
Peters, A., 2009. The effects of normal aging on myelinated nerve fibers in monkey central nervous system. Front. Neuroanat. doi:10.3389/neuro.05.011.2009.
Peters, A., 2002. The effects of normal aging on myelin and nerve fibers: A review. J. Neurocytol. doi:10.1023/A:1025731309829.
Pfefferbaum, A., Rohlfing, T., Rosenbloom, M.J., Chu, W., Colrain, I.M., Sullivan, E.V., 2013. Variation in longitudinal trajectories of regional brain volumes of healthy men and women (ages 10 to 85years) measured with atlas-based parcellation of MRI. Neuroimage doi:10.1016/j.neuroimage.2012.10.008.
Piredda, G.F., Hilbert, T., Canales-Rodríguez, E.J., Pizzolato, M., von Deuster, C., Meuli, R., Pfeuffer, J., Daducci, A., Thiran, J.-P.P., Kober, T., 2021. Fast and high-resolution myelin water imaging: Accelerating multi-echo GRASE with CAIPIRINHA. Magn. Reson. Med. 85, 209–222. doi:10.1002/mrm.28427.
Prasloski, T., Mädler, B., Xiang, Q.S., MacKay, A., Jones, C., 2012a. Applications of stimulated echo correction to multicomponent T2 analysis. Magn. Reson. Med. doi:10.1002/mrm.23157.
Prasloski, T., Rauscher, A., MacKay, A.L., Hodgson, M., Vavasour, I.M., Laule, C., Mädler, B., 2012b. Rapid whole cerebrum myelin water imaging using a 3D GRASE sequence. Neuroimage doi:10.1016/j.neuroimage.2012.06.064.
Regan, J.C., Partridge, L., 2013. Gender and longevity: Why do men die earlier than women? Comparative and experimental evidence. Best Pract. Res. Clin. Endocrinol. Metab. doi:10.1016/j.beem.2013.05.016.
Saito, N., Watanabe, M., Sakai, O., Jara, H., 2012. Human lifespan age-related changes of the brain proton density by quantitative MRI. In: Proceedings of the 20th Annual Meeting of ISMRM. Melbourne, p. 780.
Salvador, R., Verdolini, N., Garcia-Ruiz, B., Jiménez, E., Sarró, S., Vilella, E., Vieta, E., Canales-Rodríguez, E.J., Pomarol-Clotet, E., Voineskos, A.N., 2020. Multivariate brain functional connectivity through regularized estimators. Front. Neurosci. 14. doi:10.3389/fnins.2020.569540.
Smith, C.D., Chebrolu, H., Wekstein, D.R., Schmitt, F.A., Markesbery, W.R., 2007. Age and gender effects on human brain anatomy: a voxel-based morphometric study in healthy elderly. Neurobiol. Aging 28, 1075–1087. doi:10.1016/j.neurobiolaging.2006.05.018.
Smith, S.M., Jenkinson, M., Woolrich, M.W., Beckmann, C.F., Behrens, T.E.J., Johansen-Berg, H., Bannister, P.R., De Luca, M., Drobnjak, I., Flitney, D.E., Niazy, R.K., Saunders, J., Vickers, J., Zhang, Y., De Stefano, N., Brady, J.M., Matthews, P.M., 2004. Advances in functional and structural MR image analysis and implementation as FSL. in: Neuroimage S208–S219. doi:10.1016/j.neuroimage.2004.07.051, doi:S1053-8119(04)00393-3 [pii].
Smith, S.M., Nichols, T.E., 2009. Threshold-free cluster enhancement: addressing problems of smoothing, threshold dependence and localisation in cluster inference. Neuroimage. 44, 83–98. doi:10.1016/j.neuroimage.2008.03.061, doi:S1053-8119(08)00297-8 [pii].
Sowell, E.R., Peterson, B.S., Kan, E., Woods, R.P., Yoshii, J., Bansal, R., Xu, D., Zhu, H., Thompson, P.M., Toga, A.W., 2007. Sex differences in cortical thickness mapped in 176 healthy individuals between 7 and 87 years of age. Cereb. Cortex. doi:10.1093/cercor/bhl066.
Tzourio-Mazoyer, N., Landeau, B., Papathanassiou, D., Crivello, F., Etard, O., Delcroix, N., Mazoyer, B., Joliot, M., 2002. Automated anatomical labeling of activations in SPM using a macroscopic anatomical parcellation of the MNI MRI single-subject brain. Neuroimage. 15, 273–289. doi:10.1006/nimg.2001.0978S1053811901909784, [pii].
Webb, S., Munro, C.A., Midha, R., Stanisz, G.J., 2003. Is multicomponent T2 a good measure of myelin content in peripheral nerve? Magn. Reson. Med. 49, 638–645. doi:10.1002/mrm.10411.
Westerhausen, R., Walter, C., Kreuder, F., Wittling, R.A., Schweiger, E., Wittling, W., 2003. The influence of handedness and gender on the microstructure of the human corpus callosum: A diffusion-tensor magnetic resonance imaging study. Neurosci. Lett. doi:10.1016/j.neulet.2003.07.011.
Whittall, K.P., MacKay, A.L., Graeb, D.A., Nugent, R.A., Li, D.K.B.B., Paty, D.W., 1997. In vivo measurement of T2 distributions and water contents in normal human brain. Magn. Reson. Med. 37, 34–43. doi:10.1002/mrm.1910370107.
Yeatman, J.D., Wandell, B.A., Mezer, A.A., 2014. Lifespan maturation and degeneration of human brain white matter. Nat. Commun. 5, 1–12. doi:10.1038/ncomms5932.
Yu, T., Canales-Rodríguez, E.J., Pizzolato, M., Piredda, G.F., Hilbert, T., Fischi-Gomez, E., Weigel, M., Barakovic, M., Bach Cuadra, M., Granziera, C., Kober, T., Thiran, J.P., 2021. Model-informed machine learning for multi-component T2 relaxometry. Med. Image Anal. 69, 101940. doi:10.1016/j.media.2020.101940.
Zaidi, Z.F., 2010. Gender differences in human brain: a review. Open Anat. J. 2, 37–55. doi:10.2174/1877609401002010037.
Zhang, H., Schneider, T., Wheeler-Kingshott, C.A., Alexander, D.C., 2012. NODDI: practical in vivo neurite orientation dispersion and density imaging of the human brain. Neuroimage. 61, 1000–1016. doi:10.1016/j.neuroimage.2012.03.072.
Zhang, Y., Brady, M., Smith, S., 2001. Segmentation of brain MR images through a hidden Markov random field model and the expectation-maximization algorithm. IEEE Trans. Med. Imaging. doi:10.1109/42.906424.